VOLUME 122, NUMBER 46
NOVEMBER 22, 2000

JOURNAL
OF THE
AMERICAN
CHEMICAL
SOCIETY

Kinetics of Propylene Polymerization Using Bis(2-phenylindenyl)zirconium Dichloride/Methylaluminoxane

**Shirley Lin,[†] Christopher D. Tagge,[†,‡] Robert M. Waymouth,*,[†] Márcio Nele,[§,⊥]
Scott Collins,[§] and J. C. Pinto[∥]**

*Contribution from the Department of Chemistry, Stanford University, Stanford, California 94305,
Department of Chemistry, University of Waterloo, 200 University Avenue West,
Waterloo, Ontario, Canada N2L 3G1, and Programa de Engenharia Química/COPPE,
Universidade Federal do Rio de Janeiro, Rio de Janeiro, Brazil*

Received June 5, 2000

Abstract: The kinetics of propylene polymerization in toluene solution by bis(2-phenylindenyl)zirconium dichloride/methylaluminoxane at 20 °C were investigated. As the structure and properties of elastomeric polypropylenes produced by these catalysts depend sensitively on the reaction conditions, a detailed study of the kinetics was carried out to evaluate the influence of these parameters on the polymerization behavior. Studies of the solubilities and mass-transfer rates reveal that dissolved atactic polypropylene has little effect on propylene solubility but influences the mass-transfer rate of propylene into solution. The rates of propylene polymerization reach a maximum after 10−20 min and then decrease. The decrease in rate over time is faster at higher monomer concentrations. Catalyst activity was negligible at $[Al]/[Zr] = 1000$ but constant from $[Al]/[Zr] = 2500$ to $[Al]/[Zr] = 10\,000$. Analysis of molecular weights as a function of monomer concentration reveal β-hydride elimination to be the primary chain-transfer mechanism. Narrow molecular weight distributions ($M_w/M_n = 2.0{-}2.6$) were obtained. The increase of the isotactic dyads and pentads ([m] and [mmmm]) with increasing monomer concentration reveals an additional kinetic event which competes with the stereodifferentiating olefin insertion step. Modeling studies are more consistent with a mechanism involving interconversion of the catalyst between isospecific and aspecific states than a mechanism involving epimerization of the stereogenic centers of the growing polymer chain.

Introduction

Kinetics yield considerable insight into the mechanism of catalytic reactions. The recent interest in homogeneous catalytic systems for the polymerization of α-olefins has led to the kinetic investigation of many different metallocenes.[1−15] The complex dependence of the polymerization rate on time (i.e., the rate is initially fast and then decreases gradually to a steady-state value) is common to many types of olefin polymerization catalysts, including metallocenes.[1,16] A variety of proposals have been

---

[†] Stanford University.

[‡] Current address: SRI International, 333 Ravenswood Avenue, Menlo Park, CA 94025-3493.

[§] University of Waterloo.

[⊥] Current address: Programa de Engenharia Química/COPPE, Universidade Federal do Rio de Janeiro, Rio de Janeiro Brazil.

[∥] Universidade Federal do Rio de Janeiro.

(1) Brintzinger, H. H.; Fischer, D.; Mulhaupt, R.; Rieger, B.; Waymouth, R. M. *Angew. Chem., Int. Ed. Engl.* **1995**, *34*, 1143−70.

(2) Resconi, L.; Cavallo, L.; Fait, A.; Piemontesi, F. *Chem. Rev.* **2000**, *100*, 1253−1346.

(3) Fischer, D.; Mulhaupt, R. *J. Organomet. Chem.* **1991**, *417*, C7−C11.

(4) Fischer, D. Thesis, Universität Freiburg, Germany, 1992.

(5) Huang, J.; Rempel, G. L. *Ind. Eng. Chem. Res.* **1997**, *36*, 1151−1157.

10.1021/ja002003h CCC: $19.00

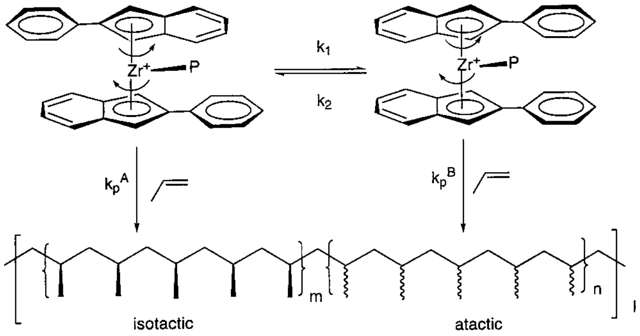

Figure 1. Proposed mechanism for the formation of stereoblock PP by (2-PhInd)$_2$ZrCl$_2$/MAO.

forwarded to explain the decrease in polymerization rate with time.[2,3,12] The complex time dependence of the rate has complicated attempts to establish the reaction order in olefin[6,8,10,11,17] and has led to some debate on the molecularity of the olefin insertion step.[2,18]

Previous investigations of the mechanism of propylene polymerization by unbridged bis(2-arylindenyl)zirconium dichloride ((2-ArInd)$_2$ZrCl$_2$) activated with methylaluminoxane (MAO) have led to the proposal of a kinetic model (Figure 1) where the rate of monomer enchainment is competitive with isomerization of the catalyst between two states which exhibit different stereoselectivities.[19−39] The differences in catalyst productivity and molecular weight (MW) and the microstructure of the polypropylenes (PPs) formed by (2-ArInd)$_2$ZrCl$_2$ with variations in ligand structure,[20,21,26,28,29] metal,[22] and polymerization conditions[19,22] have been investigated but are difficult to predict in the absence of a more complete kinetic model. An understanding of the kinetic behavior of the parent system bis(2-phenylindenyl)zirconium dichloride ((2-PhInd)$_2$ZrCl$_2$) would assist in the interpretation of past work and aid in designing new catalysts.

A common method of measuring the kinetics of olefin polymerization is to monitor monomer consumption during solution polymerization. The concentration of monomer in the liquid phase is dependent upon not only the solubility of the gas in the solvent but also the rate of mass transfer across the gas−liquid interface relative to the rate of the polymerization.[40−42] Accurate knowledge of the propylene concentration is necessary to evaluate the kinetics of the polymerization reaction. Presented here are rate versus time profiles for (2-PhInd)$_2$ZrCl$_2$/MAO at varying monomer, catalyst, and aluminum concentrations. Propylene solubilities and diffusion rates into toluene solution were measured such that monomer concentrations during the polymerization could be determined. The polymers produced in this study were analyzed to determine the role of monomer concentration in affecting MW and polymer tacticity.

Results

The rates of propylene polymerization were measured by monitoring propylene consumption from reservoirs of known volume at room temperature (see the Experimental Section). Precautions were taken to ensure that the monomer concentration in the toluene solution during the polymerization was constant and approximately equal to the saturation concentration of propylene in toluene at a given partial pressure of propylene. The metallocene dichloride was introduced to a toluene solution of MAO saturated with propylene and the amount of metallocene adjusted such that the maximum rate of polymerization was approximately an order of magnitude less than the gas diffusion rates measured for 100 mL of toluene (initial volume) at 20 °C (no polymer in the solvent) to ensure that the rate of the reaction did not influence the propylene concentration through mass-transfer effects.[40] Accordingly, the solubility of

---

(6) Jungling, S.; Mulhaupt, R.; Stehling, U.; Brintzinger, H. H.; Fischer, D. *J. Polym. Sci., Part A: Polym. Chem.* **1995**, *33*, 1305−1317.

(7) Jungling, S.; Mulhaupt, R.; Stehling, U.; Brintzinger, H. B.; Fischer, D.; Langhauser, F. *Macromol. Symp.* **1995**, *97*, 205−216.

(8) Resconi, L.; Fait, A.; Piemontesi, F. *Macromolecules* **1995**, *28*, 6667−76.

(9) Stehling, U.; Diebold, J.; Kirsten, R.; Roll, W.; Brintzinger, H. H.; Jungling, S.; Mulhaupt, R.; Langhauser, F. *Organometallics* **1994**, *13*, 964−970.

(10) Fink, G.; Herfert, N.; Montag, P. *Ziegler Catalysts*; Springer-Verlag: Berlin, 1995.

(11) Ewen, J. A.; Elder, M. J.; Jones, R. L.; Curtis, S.; Cheng, H. N. In *Catalytic Olefin Polymerization, Studies in Surface Science and Catalysis*; Keii, T., Soga, K., Eds.; Elsevier: New York, 1990; p 439.

(12) Wester, T. S.; Johnsen, H.; Kittilsen, P.; Rytter, E. *Macromol. Chem. Phys.* **1998**, *199*, 1989−2004.

(13) Busico, V.; Cipullo, R.; Esposito, V. *Macromol. Rapid Commun.* **1999**, *20*, 116−121.

(14) Chien, J. C.; Yu, Z.; Marques, M. M.; Flores, J. C.; Rausch, M. D. *J. Polym. Sci., Part A: Polym. Chem.* **1998**, *36*, 319−328.

(15) Charpentier, P. A.; Zhu, S.; Hamielec, A. E.; Brook, M. A. *Ind. Eng. Chem. Res.* **1997**, *36*, 5074−5082.

(16) Pino, P.; Mulhaupt, R. *Angew. Chem., Int. Ed. Engl.* **1980**, *19*, 857−875.

(17) Hagihara, H.; Shiono, T.; Ikeda, T. *Macromol. Rapid Commun.* **1999**, *20*, 200−202.

(18) Ystenes, M. *Makromol. Chem., Macromol. Symp.* **1993**, *66*, 71−81.

(19) Coates, G. W.; Waymouth, R. M. *Science* **1995**, *267* (5195), 217−19.

(20) Hauptman, E.; Waymouth, R. M. *J. Am. Chem. Soc.* **1995**, *117*, 11586−11587.

(21) Petoff, J. L. M.; Bruce, M. D.; Waymouth, R. M.; Masood, A.; Lal, T. K.; Quan, R. W.; Behrend, S. J. *Organometallics* **1997**, *16*, 5909−5916.

(22) Bruce, M. D.; Coates, G. W.; Hauptman, E.; Waymouth, R. M.; Ziller, J. W. *J. Am. Chem. Soc.* **1997**, *119*, 11174−11182.

(23) Kravchenko, R.; Masood, A.; Waymouth, R. M. *Organometallics* **1997**, *16*, 3635−3639.

(24) Bruce, M. D.; Waymouth, R. M. *Macromolecules* **1998**, *31*, 2707−2715.

(25) Petoff, J. L. M.; Agoston, T.; Lal, T. K.; Waymouth, R. M. *J. Am. Chem. Soc.* **1998**, *120*, 11316−11322.

(26) Lin, S.; Hauptman, E.; Lal, T. K.; Waymouth, R. M.; Quan, R. W.; Ernst, A. B. *J. Mol. Catal., A* **1998**, *136*, 23−33.

(27) Kravchenko, R.; Masood, A.; Waymouth, R. M.; Myers, C. L. *J. Am. Chem. Soc.* **1998**, *120*, 2039−2046.

(28) Tagge, C. D.; Kravchenko, R. L.; Lal, T. K.; Waymouth, R. M. *Organometallics* **1999**, *18*, 380−388.

(29) Witte, P.; Lal, T. K.; Waymouth, R. M. *Organometallics* **1999**, *18*, 4147−4155.

(30) Lin, S.; Waymouth, R. M. *Macromolecules* **1999**, *32*, 8283−8290.

(31) Nele, M.; Collins, S.; Dias, M. L.; Pinto, J. C.; Lin, S.; Waymouth, R. M. Submitted for publication.

(32) Coleman, B. D.; Fox, T. G. *J. Polym. Sci., Part A: Polym. Chem.* **1963**, *1*, 3183−3197.

(33) Coleman, B. D.; Fox, T. G. *J. Chem. Phys.* **1963**, *38*, 1065−1075.

(34) Knickmeier, M.; Erker, G.; Fox, T. *J. Am. Chem. Soc.* **1996**, *118*, 9623−9630.

(35) Knuppel, S.; Faure, J.-L.; Erker, G.; Kehr, G.; Nissinen, M.; Frohlich, R. *Organometallics* **2000**, *19*, 1262−1268.

(36) Babkina, O. N.; Bazhenova, T. A.; Bravaya, N. M.; Strelets, V. V.; Antipin, M. Y.; Lysenko, K. A. *Russ. Chem. Bull.* **1996**, *45*, 1458−1465.

(37) Bazhenova, T. A.; Antipin, M. Y.; Babkina, O. N.; Bravaya, N. M.; Lyssenko, K. A.; Strelets, V. V. *Russ. Chem. Bull.* **1997**, *46*, 2048−2052.

(38) Lee, G. Y.; Xue, M.; Kang, M. S.; Kwon, O. C.; Yoon, J. S.; Lee, Y. S.; Kim, H. S.; Lee, H.; Lee, I. M. *J. Organomet. Chem.* **1998**, *558*, 11−18.

(39) Yoon, J. S.; Lee, Y. S.; Park, E. S.; Lee, I. M.; Park, D. K.; Jung, S. O. *Eur. Polym. J.* **2000**, *36*, 1271−1275.

(40) Sun, Y. K.; Landau, R. N.; Wang, J.; LeBlond, C.; Blackmond, D. G. *J. Am. Chem. Soc.* **1996**, *118*, 1348−1353.

(41) Floyd, S.; Hutchinson, R. A.; Ray, W. H. *J. Appl. Polym. Sci.* **1986**, *32*, 5451−5479.

(42) Kittilsen, P.; Togersen, R.; Rytter, E.; Svendsen, H. In *Metalorganic Catalysts for Synthesis and Polymerization*; Kaminsky, W., Ed.; Springer-Verlag: Berlin, 1999; pp 641−650.

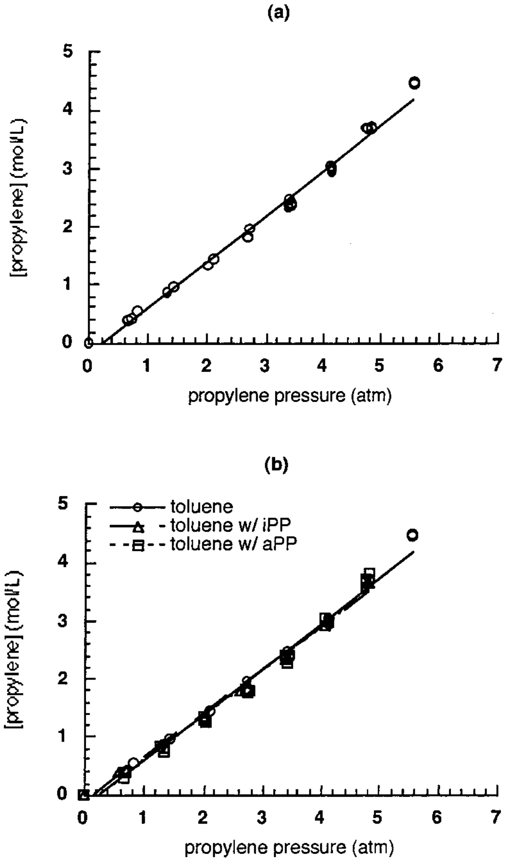

Figure 2. (a) Propylene solubility versus the partial pressure of propylene in toluene at 293 K. (b) Comparison of propylene solubility in toluene, toluene with isotactic PP, and toluene with atactic PP.

propylene in toluene and the mass-transfer rates of the monomer into solution were measured prior to the polymerization experiments being conducted.

Solubility and Mass-Transfer Rates of Propylene in Toluene at 20 °C. The solubility of propylene gas in toluene at 20 °C was measured using a method described by Deimling[43] in the range of 0−3.8 atm of propylene partial pressure by incrementally increasing the pressure over the toluene solution by ~0.68 atm and measuring the pressure drop in a propylene reservoir (see the Experimental Section). The increase in volume of toluene was measured by conducting the solubility experiment in a calibrated glass pressure bottle and noting the volume of solution when propylene consumption had ceased. The correlation between the increase in solvent volume and propylene pressure was plotted and approximated by a polynomial equation.

The relationship of solubility to propylene partial pressure for toluene at 20 °C is shown in Figure 2a. The solubility is linear with respect to pressure in the range measured for all three temperatures and decreases with increasing temperature. At 20 °C and a pressure range of 0−5.8 atm, the concentration of propylene varies from 0 to 4.34 ± 0.09 mol/L. These values are in good agreement with the mole fractions of propylene in toluene calculated by Collins[44] and the solubilities reported by Busico (±2%).[45,46]

Figure 2b compares the relationship between propylene pressure and solubility for three solutions: toluene, toluene with

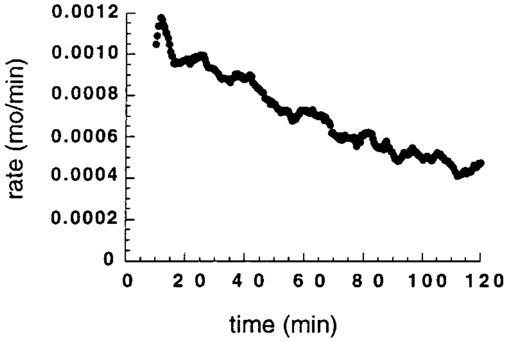

Figure 3. Representative kinetic profile for propylene polymerization using $(2\text{-PhInd})_2ZrCl_2$/MAO.

4 g of isotactic PP ([mmmm] = 90%, M_n = 35 700, M_w = 71 300), and toluene with 4 g of atactic PP ([mmmm] = 10%, M_n = 233 000, M_w = 486 000). The solubility of propylene in toluene does not change with up to 4 g of polymer suspended or dissolved in the solution.

The mass-transfer coefficients of propylene into toluene at the three temperatures were calculated according to eq 1,[43]

$$\frac{P_2 - P_0}{P_1 - P_0}\ln\frac{P_1 - P_2}{P_t - P_2} = k_L a t \qquad (1)$$

where P_1 = initial pressure in the reservoir, P_2 = final pressure in the reservoir, P_0 = presaturation pressure, P_t = pressure at time t, and $k_L a' = V k_L a$, where $k_L a$ is the mass transport coefficient and V is the volume of the solution. The change in propylene concentration with time (diffusion rate) is then defined as

$$\mathrm{d[propylene]/d}t = k_L a(C^* - C_L) \qquad (2)$$

where C^* is the equilibrium concentration of propylene at a given pressure and C_L is the actual concentration. All mass-transfer coefficients were measured for a difference of ~0.68 atm increase in propylene overpressure in the reactor. This step in pressure was chosen since it was a pressure differential large enough to result in a substantial difference in $C^* - C_L$ (0.5 M at 20 °C) but not so large as to cause gas absorption by the solution before the stirring is commenced (see the Experimental Section).

The average values of $k_L a$ found for propylene dissolving in 100 mL of toluene (initial volume) in a 300 mL stainless steel reactor equipped with a mechanical stirrer (1460 rpm) at 20 °C ranged from 1.4 to 10 s^{-1} (see the Supporting Information). As the volume of toluene solution increased with increasing propylene pressure, $k_L a$ decreased. The $k_L a$ values decreased by 3−4-fold in the presence of 4 g of atactic PP. In contrast, values for $k_L a$ are insensitive to the presence of up to 4 g of isotactic PP (Supporting Information). The lower value of $k_L a$ in the presence of atactic PP is likely a consequence of the greater viscosity of toluene solutions containing dissolved atactic PP.

Kinetic Behavior of $(2\text{-PhInd})_2ZrCl_2$. A representative kinetic profile for propylene polymerization by $(2\text{-PhInd})_2ZrCl_2$ is shown in Figure 3. The plot reveals that there is a complex rate dependence on time where the rate decreases with increasing time after reaching a maximum at 10−20 min. A decrease in

---

(43) Deimling, A.; Karadikar, B. M.; Shah, Y. T. *Chem. Eng. J.* **1984**, *29*, 127−140.

(44) Bravakis, A.; Bailey, L.; Pigeon, M.; Collins, S. *Macromolecules* **1998**, *31*, 1000−1009.

(45) Busico, V.; Brita, D.; Caporaso, L.; Cipullo, R.; Vacatello, M. *Macromolecules* **1997**, *30*, 3971−3977.

(46) As pointed out by a reviewer, calculated values for the solubility of propylene in toluene can depend on the type of equation of state used. See: Atiqullah, M., Hassan, H., Hamid, H. *Eur. Polym. J.* **1998**, *34*, 1511−1520.

Table 1. Propylene Polymerization at Four Monomer Concentrations[a]

entry	pressure (atm)	pressure (psig)	[propylene] (mol/L)	amt of propylene consumed (g)	amt of polymer recovered (g)	$r_{\max}$ (mmol/min)	productivity [(kg of PP/ mol of Zr)/h]	M_n[d]	M_w[d]	M_w/M_n
1[b]	1.68	10	1.16	1.14	1.07	0.442	4 652	29 000	59 300	2.0
2[c]	1.68	10	1.16	1.28	1.22	0.546	5 304	30 000	61 600	2.0
3[b]	3.04	30	2.22	2.21	2.14	0.672	8 295	43 300	87 900	2.0
4[c]	3.04	30	2.22	2.70	2.53	0.831	9 806	43 100	90 000	2.1
5[b]	3.72	40	2.75	2.70	2.51	0.746	9 094	55 400	117 000	2.1
6[c]	3.72	40	2.75	3.09	2.70	0.921	9 782	59 600	125 000	2.1
7[b]	5.08	60	3.81	4.17	4.08	1.65	12 216	66 700	143 000	2.1
8[c]	5.08	60	3.81	5.08	5.01	1.83	15 000	72 500	164 000	2.3
9[e]	bulk	bulk	~11		2.92		19 467	96 600	236 000	2.4

[a] Conditions: $[Zr] = 1.0 \times 10^{-6}$ M; $[Al] = 3.16$ ¥ 10^{-2} M; $T = 293$ K; $t_{rxn} = 120$ min. [b] Same catalyst solution used over 2 days. [c] Same catalyst solution (different from that in footnote *b*) used over 2 days. [d] Determined by high-temperature GPC versus PP standards. [e] $t_{rxn} = 90$ min.

Table 2. Propylene Polymerization at 3.04 atm of Propylene (30 psig) with Four Catalyst Concentrations[a]

entry	[Zr] (mol/L) ($\times 10^7$)	[Al]/[Zr]	amt of propylene consumed (g)	amt of polymer recovered (g)	$r_{\max}$ (mmol/ min)	productivity [(kg of PP/ mol of Zr)/h]	M_n[d]	M_w[d]	M_w/M_n	[m][e] (%)	[mmmm][e] (%)
1[b]	5	63 200	1.45	1.32	0.501	10 232	44 700	94 500	2.1	62	20
2[c]	5	63 200	0.87	0.73	0.368	5 659	40 300	88 200	2.2	62	21
3[b]	10	31 600	2.08	1.82	0.815	7 054	52 900	109 000	2.1	63	21
4[c]	10	31 600	2.43	2.23	0.787	8 643	45 600	100 000	2.2	61	19
5[b]	15	21 100	3.48	3.14	1.19	8 113	56 100	124 000	2.2	62	20
6[c]	15	21 100	2.76	2.55	0.776	6 589	51 200	110 000	2.2	60	19
7[b]	20	15 800	3.81	3.54	1.36	6 860	62 500	130 000	2.1	61	20
8[c]	20	15 800	3.53	3.34	1.18	6 472	48 600	107 000	2.2	61	19

[a] Conditions: [propylene] = 2.22 M; $[Al] = 3.16 \times 10^{-2}$ M; $T = 293$ K; $t_{rxn} = 120$ min. [b] Same catalyst solution used over 2 days. [c] Same catalyst solution (different from that in footnote *b*) used over 2 days. [d] Determined by high-temperature GPC versus PP standards. [e] Determined by ^{13}C NMR.

polymerization rate over time is seen for all the experiments reported. Propylene polymerizations were conducted at four monomer concentrations at 20 °C. The polymerization at each monomer concentration was repeated twice to test reproducibility. The concentrations of zirconocene and MAO were kept constant by correcting for the volume increase in the toluene solution with addition of propylene. The ratio of MAO to catalyst was high ([Al]/[Zr] = 31 600) because a minimum of 200 mg of MAO was necessary to remove impurities from the reactor and obtain a reasonable activity.

The results from the two sets of polymerizations conducted for a range of propylene concentrations (1.16−3.81 M) are shown in Table 1. Entries 1 and 2, 3 and 4, 5 and 6, and 7 and 8 were duplicate polymerizations of each other. The amount of polymer obtained from each one differed by 0.15−1.0 g. However, entries 1, 3, 5, and 7 and entries 2, 4, 6, and 8 were conducted with two different catalyst stock solutions, and it is likely that the discrepancy in the amount of polymer obtained arises from the ability to accurately measure out such small quantities of metallocene.[47]

The rates of polymerization for entries 1−8 were calculated by determining the number of moles consumed between time *t* min and $t - 10$ min from the drop in the pressure of the reservoir used and dividing that number by 10 min. The maximum rate of polymerization and the productivity for each polymerization are reported in Table 1. The maximum rate occurred 10−20 min after injection of the catalyst, and this rate increased with increasing monomer concentration. The decrease in rate with time was also dependent on monomer concentration. The rate of deactivation at 3.8 M is faster than at 1.2 M.

Propylene polymerizations at 2.22 M propylene (3.04 atm = 30 psig) were conducted at four different initial zirconium concentrations. The concentration of Al was kept constant for all polymerizations ($[Al] = 3.16 \times 10^{-2}$ M). The initial [Zr] was varied from 5.0×10^{-7} to 2.0×10^{-6} M. Table 2 contains the data from eight polymerizations. Figure 4 shows the kinetic profile of entries 2 and 8 in Table 2. The maximum activity is reached within 10−20 min of catalyst injection and then decreases over the rest of the polymerization. The rate at which polymerization activity decreases is independent of the initial [Zr].

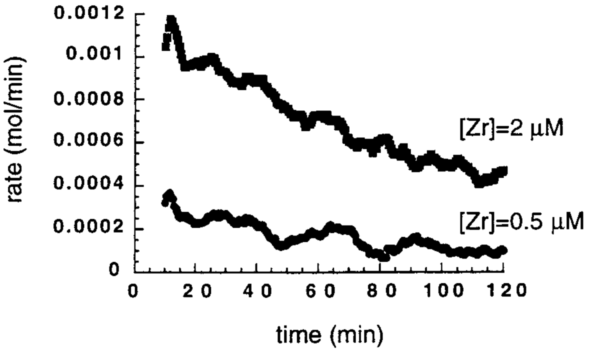

Figure 4. Rate versus time profiles for propylene polymerizations at varying catalyst concentrations (entries 5 and 8 of Table 2).

The dependence of the rate on [Al] was investigated by conducting propylene polymerizations at 3.04 atm (30 psig) with four different MAO concentrations. The amount of metallocene was kept constant at 1.41×10^{-5} M. For these experiments, the [Zr] was increased by an order of magnitude from the concentrations used in the other polymerizations to keep the amount of MAO being used greater than 100 mg. Table 3 contains the data for the four polymerizations conducted. To keep the amount of polymer being made close to 4 g, the polymerizations with [Al]/[Zr] = 2500 and 5000 were run for 90 min and the polymerization with [Al]/[Zr] = 10 000 was

---

(47) For example, a 1.0 g difference in the amount of polymer made for two different polymerizations at 5.08 atm (60 psig) over 120 min could arise from as little as a 2 μg difference in the amount of catalyst used (based on the productivity calculated from entry 7).

Table 3. Propylene Polymerization at 3.04 atm of Propylene (30 psig) with Three MAO Concentrations[a]

entry	t_{rxn} (min)	[Al] (mM)	[Al]/[Zr]	amt of propylene consumed (g)	amt of polymer recovered (g)	r_{max} (mmol/ min)	productivity [(kg of PP/ mol of Zr)/h]	M_n[d]	M_w[d]	M_w/ M_n	[m][e] (%)	[mmmm][e] (%)
1[b]	120	14	1 000	0.54	0.34	0.462	93.5	31 300	78 900	2.5	66	27
2[c]	90	35	2 500	5.94	6.30	3.5	2309	63 200	155 000	2.4	64	24
3[b]	90	70	5 000	5.93	6.26	3.88	2294	63 900	162 000	2.5	65	24
4[b]	60	140	10 000	5.09	5.27	4.57	2897	53 100	138 000	2.6	64	25

[a] Conditions: [propylene] = 2.22 M; [Zr] = 1.41×10^{-5} M; $T = 293$ K. [b] Same catalyst solution used over 2 days. [c] Different catalyst solution from that in footnote *b*. [d] Determined by high-temperature GPC versus PP standards. [e] Determined by ^{13}C NMR.

Table 4. Pentad Distribution and ΔH_f for Propylene Polymerizations at Various Monomer Concentrations

entry[a]	[propylene] (mol/ L)	[m]	[mmmm]	[mmmr]	[rmmr]	[mmrr]	[mmrm] + [rmrr]	[mrmr]	[rrrr]	[mrrr]	[mrrm]	ΔH_f[c] (J/ g)
1	1.16	0.57	0.15	0.15	0.06	0.13	0.20	0.11	0.05	0.09	0.07	2.6
2	1.16	0.58	0.15	0.14	0.06	0.15	0.19	0.10	0.05	0.09	0.06	nd[d]
3	2.22	0.61	0.19	0.15	0.06	0.13	0.18	0.11	0.04	0.08	0.07	5.3
4	2.22	0.62	0.21	0.15	0.05	0.14	0.18	0.10	0.03	0.07	0.06	nd
5	2.75	0.63	0.22	0.16	0.06	0.14	0.17	0.09	0.03	0.07	0.06	nd
6	2.75	0.64	0.23	0.16	0.05	0.14	0.18	0.09	0.03	0.07	0.06	nd
7	3.81	0.65	0.24	0.15	0.06	0.13	0.17	0.09	0.03	0.07	0.06	nd
8	3.81	0.65	0.25	0.15	0.05	0.13	0.17	0.09	0.03	0.07	0.05	8.5
9[b]	11	0.69	0.30	0.16	0.05	0.11	0.17	0.08	0.03	0.05	0.04	21.9

[a] Entry numbers correspond to the entry numbers in Table 1. [b] Synthesized in liquid propylene, 20 °C, [Zr] = 1.0×10^{-6} M; [Al] = 3.16×10^{-2} M, t_{rxn} = 95 min. [c] Determined by DSC. [d] Not determined.

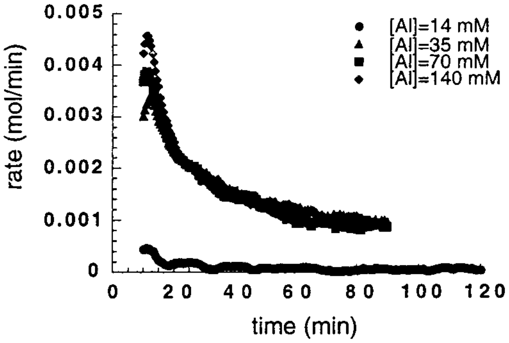

Figure 5. Rate of polymerization versus time at various [Al]/[Zr] ratios.

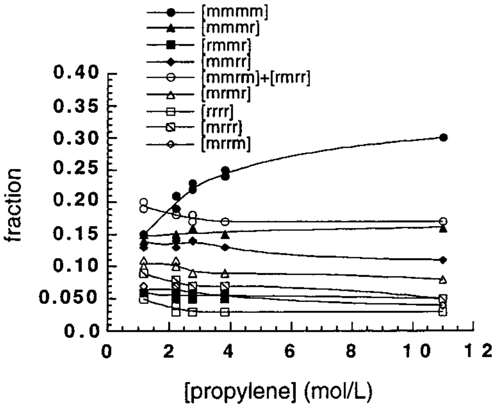

Figure 6. Pentad distribution versus monomer concentration for entries 1−9 of Table 4.

run for 60 min, instead of 120 min. There is little difference in activity among [Al]/[Zr] = 2500, [Al]/[Zr] = 5000, and [Al]/[Zr] = 10 000 (Table 3 and Figure 5). However, the rate of polymerization is very slow at [Al]/[Zr] = 1000 ([Al] = 14 mM = 100 mg of MAO). The low activity observed is likely due to the amount of MAO being insufficient to remove all the impurities from the reactor system.

Influence of Polymerization Conditions on Polymer Structure. The MWs of polymers synthesized with (2-PhInd)$_2$ZrCl$_2$/MAO increased with increasing monomer concentrations, M_n = 30 000−72 000 and M_w = 60 000−164 000 (Table 1). In contrast, M_n and M_w increased with increasing [Zr] but only over a small range (Table 2). There is no clear trend in MW as a function of aluminum concentration (Table 3).

The MW distributions are characterized by polydispersity values M_w/M_n that range from 2 to 2.6. From Tables 1−3, a trend can be seen in which polydispersity increases slightly with increasing rate of polymerization (both r_{max} and productivity). Polymerizations in which the maximum rate is less than 1.6 mmol/min have polydispersities from 2 to 2.2. Broader distributions (M_w/M_n = 2.5−2.6) are seen for entries 2 and 3 in Table 3 where the maximum rates of polymerization are 3.9−4.6 mmol/min.

The tacticity of PPs synthesized with (2-PhInd)$_2$ZrCl$_2$/MAO depends on monomer concentration. As seen in Table 4, [mmmm] increases (15−30%) and [mmrm] + [rmrr] ([xmrx]) decreases as the monomer concentration increases from 1.2 to 11 M. A plot of the stereochemical pentad fractions versus monomer concentration is shown in Figure 6. There is little effect on polymer microstructure from changing the zirconium and aluminum concentrations.

Given the dependence of the polymer microstructure on monomer concentration, we also investigated the effect of monomer concentration on the thermal properties of the PP synthesized. Differential scanning calorimetry (DSC) measurements on samples synthesized with [propylene] = 1.16−11 M show a broad, multimodal melting transition from 40 to 150 °C with increasing crystallinity (ΔH_f) with increasing monomer concentration (Table 4). Figure 7 shows the DSC curves for two PPs synthesized at 2.2 and 11 M propylene (entries 3 and 9 of Table 4). Entry 3, a polymer with [mmmm] = 19%, exhibits a broad melting transition from 40 to 140 °C and ΔH_f = 5.3 J/g. Entry 9, with an [mmmm] = 30%, has a similarly broad melting transition and ΔH_f = 21.9 J/g.

Discussion

Rate of Propylene Polymerization. The polymerization rates of metallocene catalysts are typically high; at 1−2 bar of propylene pressure at room temperature, the turnover frequencies

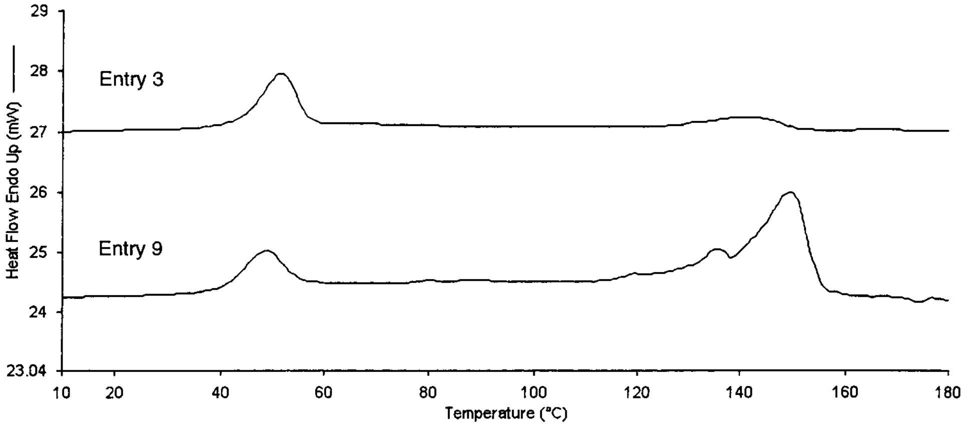

Figure 7. Comparison of DSC heating curves for entries 3 and 9 of Table 4.

for some of the more active metallocenes have been estimated at 1600 monomer insertions per second.[13] For reactions in a gas−liquid system with large rates, the rate of gas−liquid mass transfer can be competitive with the reaction rate. Blackmond and co-workers[40] have shown how mass-transfer rates relative to the rate of reaction can influence the stereochemical outcome of hydrogenation reactions. As we had previously observed a dependence of polymer stereochemistry on monomer concentration with the (2-PhInd)$_2$ZrCl$_2$/MAO catalyst, it was especially important to employ experimental conditions such that the rate of mass transfer would not interfere with interpretations of the influence of monomer concentration on the stereospecificity of these polymerization systems. The solubilities and mass-transfer rate of propylene in toluene at 20 °C were measured, and an experimental protocol was designed such that (1) the rate of propylene consumption measured is due only to polymerization, (2) the monomer concentration during polymerization is approximately equal to the saturation concentration at a given pressure, and (3) propylene conversion is $\leq$4 g such that the solubility of the monomer in the polymerization solution does not change significantly from the solubility in a toluene solution without polymer (conditions at the beginning of the polymerization).

With these criteria, we were able to conduct propylene polymerizations in toluene solution using a variety of conditions and obtain rate versus time profiles.[48] For all the polymerizations conducted, the rate was not constant over the entire time of the reaction but decreased from a maximum after 10−20 min. A decreasing rate profile is not uncommon for olefin polymerization catalysts, including metallocenes.[1,16] Several factors have been implicated as sources of deactivation for these catalysts including regioirregular propylene insertion,[30,49−52] π-allyl species,[53] and zirconocene dimers.[3] Regioirregular propylene insertions have been observed for (2-PhInd)$_2$ZrCl$_2$/MAO and have been implicated as a source of reversible inhibition for unbridged 2-arylindenyl catalysts.[30]

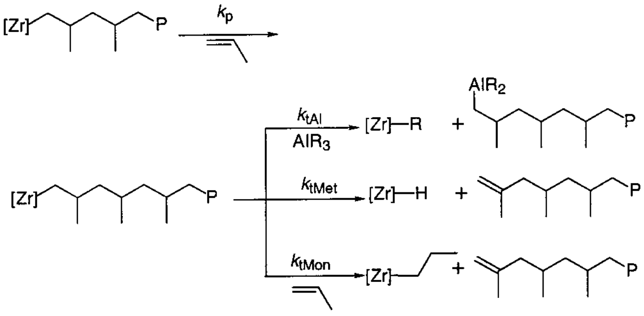

Figure 8. Mechanisms of chain transfer in (2-PhInd)$_2$ZrCl$_2$/MAO.

Another characteristic of the activity of this catalyst system is that the rate profile decreases faster with increasing monomer concentration. The source of the monomer-concentration-dependent deactivation pathway is not obvious. A possible cause is the formation of a stable allyl species, as proposed by Resconi.[53]

Due to the complex time dependence on the rate of polymerization, it is impossible to write a rate law for the polymerization that is a simple function of [Zr] and [propylene], and therefore the results of the polymerizations conducted do not provide any indication of the molecularity of the insertion event.[54] Previous studies on the kinetics of metallocene polymerization have tried to correlate maximum polymerization rate with monomer concentration;[10] however, in the absence of any measurement of the number of active sites, care must be taken in interpreting these results.[13]

Influence of [Propylene] and [Zr] on MW. In addition to providing information about the rate of polymerization, these experiments revealed the influence of monomer concentration on MW. The three most common chain-transfer mechanisms in metallocene polymerizations are chain transfer to metal (β-hydride elimination), chain transfer to monomer, and chain transfer to aluminum (Figure 8).[1,8] If chain transfer to metal and/or chain transfer to aluminum are the dominant mechanisms, there will be a dependence of MW on monomer concentration. If chain transfer to monomer is favored, the MW will be independent of monomer concentration.

---

(48) These plots (Figure 3) show slight fluctuations in rate over a period of 5 min, likely due to small changes in temperature inside the reactor and/or nonconstant propylene flow through the pressure regulator used due to the small magnitude of propylene consumption. These fluctuations are less evident for faster rates; cf. Figure 5.

(49) Busico, V.; Cipullo, R.; Corradini, P. *Makromol. Chem., Rapid Commun.* **1993**, *14*, 97−103.

(50) Busico, V.; Cipullo, R.; Corradini, P. *Makromol. Chem.* **1993**, *194*, 1079−1093.

(51) Busico, V.; Cipullo, R.; Chadwick, J. C.; Modder, J. F.; Sudmeijer, O. *Macromolecules* **1994**, *27*, 7538−43.

(52) Carvill, A.; Tritto, I.; Locatelli, P.; Sacchi, M. C. *Macromolecules* **1997**, *30*, 7056−7062.

(53) Resconi, L. *J. Mol. Catal., A* **1999**, *146*, 167−178.

(54) Nevertheless, we could approximate the rate law by examining the relationship between catalyst productivity and monomer or initial zirconium concentration. The average productivity, P_p, can be expressed as $P_p = k_p[\text{propylene}]^m[\text{zirconium}]^n$, where [Zr] is the initial zirconium concentration. The slopes of the plots of log P_p versus log [propylene] and log [Zr] should provide a crude estimate of the apparent order in monomer m and the order in zirconium n. The plots reveal that $m = 1.1$ and $n = 0.8-1.1$. These data indicate that the productivity of this catalyst is approximately first-order in monomer and initial Zr concentration.

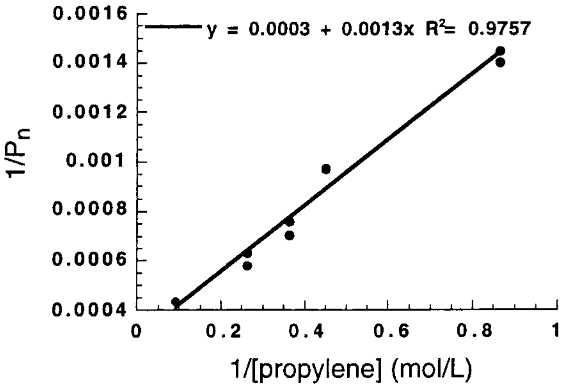

Figure 9. $1/P_n$ versus 1/[propylene] for entries 1−8 of Table 1.

The degree of polymerization, P_n (defined as M_n/(MW of propylene)), can be related to the three chain-transfer processes by eq 3,

$$P_n = \frac{k_p[\mathrm{Zr}][\mathrm{M}]}{k_{t,\mathrm{Mon}}[\mathrm{Zr}][\mathrm{M}] + k_{t,\mathrm{Met}}[\mathrm{Zr}] + k_{t,\mathrm{Al}}[\mathrm{Zr}][\mathrm{Al}]} \qquad (3)$$

$$\frac{1}{P_n} = \frac{k_{t,\mathrm{Mon}}}{k_p} + \left(\frac{k_{t,\mathrm{Al}}[\mathrm{Al}] + k_{t,\mathrm{Met}}}{k_p}\right)\frac{1}{[\mathrm{M}]} \qquad (4)$$

where the rate of propagation is assumed to be first-order in both [Zr] and [propylene]. A plot of $1/P_n$ versus 1/[propylene] will yield a line from which the relative contributions of the various chain-transfer processes ($k_{t,\mathrm{Met}} + k_{t,\mathrm{Al}}$[Al]) and $k_{t,\mathrm{Mon}}$ can be estimated.[8,9]

Figure 9 shows the plot of eq 4 using the data from Table 1. The ratio of the slope to the *y*-intercept reveals that *β*-hydride elimination and/or chain transfer to aluminum is 4 times faster than chain transfer to monomer in the monomer concentration range studied. The small variation in M_n as a function of aluminum concentration (Table 3) suggests that *β*-hydride elimination is the principle chain-transfer mechanism.[55]

The narrow polydispersities (M_w/M_n = 2.0−2.6) for the PPs synthesized here are in contrast to the values previously reported which ranged from 2.6 to 5.0 for this class of catalysts.[19,21−23,26,28,29] From comparing previous experimental protocols with the one used for this study, we conclude that the polydispersity of polymers synthesized by (2-PhInd)$_2$ZrCl$_2$/MAO is sensitive to variations in monomer concentration during the polymerization. Previous procedures used by this research group led to conditions where the initial toluene solution (75 mL) was partially saturated with monomer prior to injection of a large volume of solvent (25 mL) containing the activated catalyst, which was not saturated in monomer. This method of polymerization would lead to a monomer concentration during polymerization which was far from the saturation concentration at the given pressure; the concentration would then increase as the rate of polymerization decreased. Further changes in monomer concentration may have been caused by the synthesis of more than 4 g of polymer during a polymerization which would decrease the mass-transfer rates and possibly change the solubility of propylene in the solution.

In addition to the dependence on the experimental protocol, there appears to be a correlation between the rate of polymerization and the MW distribution, with slightly broader polydispersities at higher polymerization rates (Table 3, $r_{\max}$ = 3.9−4.6 mmol/min, M_w/M_n = 2.5−2.6, respectively). Whether this trend is general for these catalysts is not clear.

Effect of Monomer Concentration on Polymer Microstructure and Properties. The influence of monomer concentration on polymer microstructure was also examined. The isotactic pentad content ([mmmm]) increased from 15% to 30% as monomer concentration increased from 1 to 11 M (Table 4), while the dyad content [m] increased from 57% to 69%. The intensity of the remaining pentads decreased or remained relatively constant. A change in the stereospecificity of the polymerization reaction with monomer concentration is a signature for a mechanism involving a kinetic step that competes with the stereodifferentiating monomer insertion step.[40,56] We have previously proposed a Coleman and Fox type[32,33,57] two-state mechanism where the catalyst interconverts between two states exhibiting different stereospecificities (Figure 1). According to a kinetic model recently developed,[31] the pentad distribution at any particular monomer concentration will depend on three fundamental quantities: the enantiomorphic stereoselectivity α of the isospecific state, the stereoselectivity *β* of the aspecific state (either site or chain-end control for the aspecific state can be invoked), and the relative reactivity/stability of the two states given by the parameter *g*/*K* (if *g*/*K* > 1, the isospecific state is the more reactive/stable).

The response of the pentad distribution to changes in monomer concentration, for any particular values of α, *β*, and *g*/*K*, can be described by Δ, which is defined as the (average) ratio of the rates of propagation relative to the rates of interconversion (eq 5).[31]

$$\Delta = \left(\frac{k_p^{\,A}}{k_1} + \frac{k_p^{\,A}}{k_2}\right)\frac{[\mathrm{M}]}{2} \qquad (5)$$

Changes in the observed pentad distributions reported in Table 4 have been previously modeled and shown to be consistent with values of Δ ranging from ∼1 to 10 as the propylene concentration increases from 1.2 to 11 M.[31,58] Values of the other three parameters that best fit the model to the experimental data were α = 0.97, $\beta = P_r$ = 0.56 (i.e., chain-end control for the aspecific state, displaying a slight tendency for the formation of syndiotactic PP), and g/K = 0.6 (SSQ = 1.7×10^{-3}).

While the two-state kinetic model provides an adequate fit to the data, this analysis does not rule out other mechanisms that might lead to the observed change in stereospecificity with monomer concentration. Another interpretation is that epimerization of the last inserted stereocenter of the growing polymer chain[8,45] competes with olefin insertion. This has been observed for stereorigid isospecific *ansa*-metallocenes and leads to a change in stereospecificity with monomer concentration, particularly at low monomer concentrations.[8,45] In the present case, since in the limit of high monomer concentration the stereospecificity is relatively modest ([mmmm] = 0.30 at 11 M propylene), one could propose that the (2-ArInd)$_2$ZrCl$_2$/MAO catalyst system behaves as a single-state catalyst that adopts a conformation during insertion that leads to the formation of poorly isotactic PP. Alternatively, owing to the low barrier to the interconversion process observed in model studies,[22,34,59,60]

---

[55] This result is consistent with the vinylidene end group being the only unsaturated end group observed in these polymers.

[56] Landis, C. R.; Halpern, J. *J. Am. Chem. Soc.* **1987**, *109*, 1746.

[57] Cheng, H. N.; Babu, G. N.; Newmark, R. A.; Chien, J. C. W. *Macromolecules* **1992**, *25*, 6980−6987.

[58] The two-state model also predicted that M_w/M_n = 2.0 and constant over this range of Δ values. This is consistent with the observed MW distributions.

[59] Erker, G.; Aulbach, M.; Knickmeier, M.; Wingbermühle, D.; Krüger, C.; Nolte, M.; Werner, S. *J. Am. Chem. Soc.* **1993**, *115*, 4590−4601.

Table 5. Calculated Pentad Distributions from the Chain Epimerization Model with Deviations from Observed Data[a] Entry numbers correspond to entries in Tables 1 and 4

entry	ν^b	[mmmm]	[mmmr]	[rmmr]	[mmrr]	[mmrm] + [rmrr]	[mrmr]	[rrrr]	[mrrr]	[mrrm]	SSQ
1	0.68	0.15	0.15	0.05	0.15	0.19	0.10	0.05	0.10	0.08	5.6E−04
2	0.67	0.14	0.15	0.05	0.15	0.20	0.10	0.05	0.10	0.07	8.5E−04
3	0.70	0.17	0.16	0.04	0.16	0.17	0.09	0.04	0.09	0.08	1.9E−03
4	0.72	0.19	0.16	0.04	0.16	0.16	0.08	0.04	0.08	0.08	2.0E−03
5	0.73	0.21	0.16	0.04	0.16	0.16	0.08	0.04	0.08	0.08	1.9E−03
6	0.73	0.21	0.16	0.04	0.16	0.15	0.08	0.04	0.08	0.08	2.3E−03
7	0.74	0.22	0.16	0.04	0.16	0.15	0.07	0.04	0.07	0.08	3.3E−03
8	0.74	0.23	0.16	0.04	0.16	0.15	0.07	0.04	0.07	0.08	3.9E−03
9	0.77	0.27	0.17	0.03	0.17	0.12	0.06	0.03	0.06	0.08	8.6E−03

[a] Entry numbers correspond to entries in Tables 1 and 4. [b] Calculated stereoselectivity.

the catalyst might isomerize between several states, but at a rate faster than that of monomer insertion, leading to kinetic behavior similar to that of a single-state catalyst.[44,61,62] In either case, chain epimerization[8,45] would lead to a decrease in stereoregularity of the polymer with decreasing monomer concentration. Busico had derived an equation for the response of [m] to changes in [propylene] for isospecific catalysts.[45]

To address the possible role of chain epimerization, the same mass-balance kinetic approach previously developed[31] was adopted, and it was found that the pentad expressions for a single-state catalyst that polymerizes propene by a site control mechanism with interfering epimerization are given by the modified stereoselectivity parameter ν:

$$\nu = \frac{(k_p[\mathrm{M}]^n/k_e)\alpha + 1}{k_p[\mathrm{M}]^n/k_e + 2} \tag{6}$$

where k_p and k_e are the propagation and epimerization rate constants, respectively, [M] is the monomer concentration, α is the enantiomorphic-site stereoselectivity, and n is the insertion reaction order of the insertion process ($1 \leq n \leq 2$).[45] The expressions for the various pentads are then expanded in the normal way,[2,63] with ν replacing the enantiomorphic-site parameter α (for example, $[\mathrm{mmmm}] = \nu^5 + (1 - \nu)^5$).

It is instructive to analyze how the catalyst stereoselectivity (ν) responds to limiting conditions. When k_p[M] becomes large compared to k_e (e.g., at higher monomer concentrations), $\nu \rightarrow \alpha$, provided $k_p[\mathrm{M}]/k_e \gg 2$. Conversely, $\nu \rightarrow 0.5$ as $k_p[\mathrm{M}]/k_e$ approaches zero ($k_e \gg k_p[\mathrm{M}]$), and perfectly atactic PP would be produced. Therefore, the epimerization process is a valid, alternative explanation for the response of the pentad distribution to a change in monomer concentration, assuming that the catalyst behaves as a single-state catalyst (vide supra). According to this analysis, the expressions for the individual pentad intensities at any monomer concentration correspond to those expected for a site-control mechanism. Thus, the overall pentad distribution should conform to that predicted by a site-control mechanism, regardless of experimental conditions, if epimerization is the sole factor responsible for degradation of polymer stereoregularity at lower monomer concentrations.

If the calculated data are compared with the experimental data, it can be seen that, at higher monomer concentration, the observed pentad distribution deviates from that predicted from a site-control/epimerization mechanism, as shown by the increase in the residual sums of squares (Table 5). Even neglecting the experiment in liquid propylene, the fit of a site-control model to the data is, on average, 5 times worse at 3.8 M vs 1.2 M in propylene. Nevertheless, the absolute magnitude of these deviations is comparable to the errors expected in measuring experimental pentad distributions. It is therefore instructive to examine the predicted versus observed response of some of the individual pentad intensities at different C_3H_6 concentrations. The calculated intensities for the more intense pentads (i.e., mmmm, mmmr, mmrr, and xmrx) are shown in Figure 10 along with the (averaged) experimental data from Table 4. The calculated parameters corresponding to the best fit of this model over all pentads are $\alpha = 0.79$, $k_p/k_e = 2.45$ M^{-1}, and $n = 1.0$.

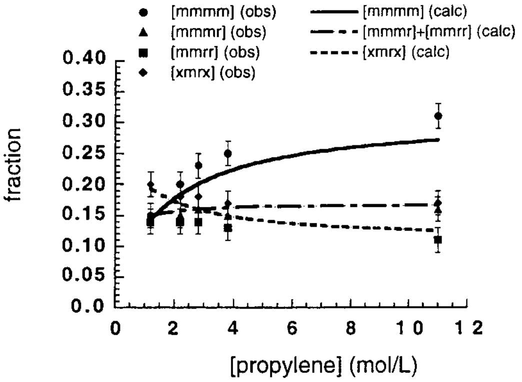

Figure 10. Experimental and calculated pentad distributions obtained for a single-state catalyst with interfering epimerization reaction ($k_p/k_e = 2.5$ M^{-1}, $\alpha = 0.79$, $n = 1.0$).

As noted previously, the overall fit degrades as the monomer concentration increases. The calculated value of the mmmm pentad is systematically lower than the experimental value, except for the polymerization at the lowest monomer concentration. More importantly, a site-control mechanism which includes epimerization predicts the same response for, e.g., the mmmr and mmrr pentads to changes in [C_3H_6] (i.e., they both have one stereoerror and are unsymmetrical), but as indicated in Figure 6, while the former pentad does change in the expected manner, the latter actually *decreases* slightly in intensity with increasing [C_3H_6]. Furthermore, they do not have the same numerical value, as predicted by the model. This analysis indicates that epimerization alone does not adequately account for the observed changes to the pentad distribution, regardless of the overall fit of the model to the data or the particular parameters employed.

As indicated above, a two-state model does account for the observed changes in the pentad distribution (in terms of both the overall fit to the data and the trends for individual pentads) with one state isospecific ($\alpha = 0.97$), the other aspecific with

---

(60) Erker, G.; Nolte, R.; Krüger, C.; Schlund, R.; Benn, R.; Grondey, H.; Mynott, R. *J. Organomet. Chem.* **1989**, *364*, 119−132.

(61) Gauthier, W. J.; Collins, S. *Macromolecules* **1995**, *28*, 3779−86.

(62) Gauthier, W. J.; Corrigan, J. F.; Taylor, N. J.; Collins, S. *Macromolecules* **1995**, *28*, 3771−8.

(63) Odian, G. *Principles of Polymerization*, 3rd ed.; John Wiley and Sons: New York, 1991.

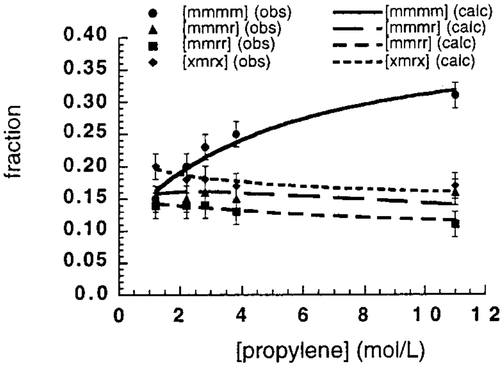

Figure 11. Experimental and calculated pentad distributions obtained for a two-state catalyst with enantiomorphic-site control on both states and interfering epimerization reaction ($\alpha = 0.96$, $\beta = 0.5$, $g/K = 0.9$, $\Delta/M = 2.7$, $k_p/k_e = 5.1\ M^{-1}$).

a slight tendency to form syndiotactic PP by a chain-end control mechanism ($P_{rac} = 0.56$), and each state contributing significantly to the PP microstructure ($g/K = 0.6$).

It is worth investigating whether the effects of competing epimerization, in combination with the basic features of a two-state model, provide a better fit to the observed data than a two-state model alone. The epimerization reaction involves reversible β-H elimination, and thus one would expect that k_p/k_e would vary in the same manner as $k_p/k_{t,Met}$ with catalyst structure/polymerization conditions. In connection with this, we note that *ansa*-metallocene analogues *rac*- and *meso*-$Me_2Si(2\text{-}PhInd)_2ZrCl_2$ have been studied in connection with modeling the behavior of unbridged catalyst 1, and it is evident from this work that these two complexes differ significantly in their $k_p/k_{t,Met}$ characteristics. We assumed that the absolute value of k_e was the same for both states, while allowing k_p^A and k_p^B to vary, which should approximate the expected behavior, and incorporated this additional feature into the two-state model.

As shown in Figure 11, a two-state model assuming enantiomorphic-site control for both states and including the effect of epimerization yields a better fit to the experimental data ($\alpha = 0.96$, $\beta = P_{rac} = 0.5$, $g/K = 0.9$, $\Delta/[M] = 2.7$, $k_p/k_e = 5.1\ M^{-1}$) than a model that invokes epimerization and a single-state catalyst. However, the fit of this model to the data ($SSQ = 9 \times 10^{-4}$) is not much better than that obtained using a two-state model where epimerization is not invoked ($SSQ = 1.7 \times 10^{-3}$), despite having one additional adjustable parameter. From a modeling perspective, it is questionable whether one needs to invoke epimerization to account for the response of the pentad distributions to changes in [propylene], and independent evidence for this process is needed.[64]

As the physical properties of PPs depend strongly on the microstructure, the crystallinity and thermal properties of the PPs produced also vary with monomer concentration. DSC scans of the polymers synthesized at various propylene concentrations revealed broad melting ranges for the polymer ($T_m = 40-160$ °C).[65] The data in Table 4 indicate that the heat of fusion, ΔH_f, increases as [mmmm] increases with increasing monomer concentration. As seen in Figure 7, mostly low-melting crystals ($T_m = 40$ °C) are formed at lower monomer concentrations, whereas at high monomer concentrations (e.g., liquid propylene) high-melting crystals ($T_m = 150$ °C) predominate. The fact that high melting points are observed for such low-tacticity PPs also provides indirect support for a blocky microstructure, although this interpretation is complicated by the compositional heterogeneity observed in related samples.[65-68]

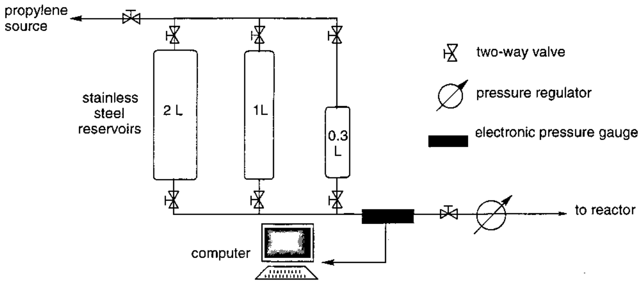

Figure 12. Schematic of the kinetics apparatus.

Conclusions

The kinetics of propylene polymerization by $(2\text{-}PhInd)_2ZrCl_2$/MAO metallocene catalysts were investigated in toluene at 20 °C. Polymerization rates increased with increasing monomer and zirconium concentrations. In addition, polymerization rates were found to reach a maximum 10−20 min after injection of metallocene and decrease over time. The activity decreased faster at higher monomer concentrations. Analysis of polymers synthesized at well-known monomer concentrations showed β-hydride elimination to be the dominant chain-transfer mechanism. Polymer polydispersities of 2.0−2.6 were obtained under these experimental conditions and indicate that the MW distributions of polymers made by $(2\text{-}PhInd)_2ZrCl_2$/MAO increase with increasing rate of polymerization. The polymer microstructure was found to be dependent on monomer concentration. This dependence was consistent with a two-state mechanism for stereoblock PP formation (Figure 1). These differences in microstructure also influenced the overall crystallinity of the polymers as determined by DSC. Further studies will focus on the temperature dependence on the rate of polymerization and polymer microstructure as well as comparison of other unbridged $(2\text{-}ArInd)_2ZrCl_2$/MAO catalysts to the parent system.

Experimental Section

All manipulations involving the metallocene and cocatalyst were carried out using standard Schlenk techniques or a nitrogen drybox.The metallocene $(2\text{-}PhInd)_2ZrCl_2$ was made according to literature procedures.[22] Polymerization grade propylene was obtained from Praxair, Matheson, or BP-Amoco and was purified through alumina/copper oxide columns. Modified methylaluminoxane (type IV) was purchased from Akzo Nobel as a solution in toluene; before use, the volatile materials were removed in vacuo to yield a powdery solid. *Caution should be taken in handling MAO as it is pyrophoric*. Toluene was purchased from Aldrich and purified through alumina/copper oxide catalyst. A 300 mL 316 stainless steel reactor or a glass Fisher-Porter bottle was used for the experiments. The maximum rate of the mechanical stirrer was determined using a stroboscope.

A schematic of the kinetics apparatus is shown in Figure 12. The apparatus consists of three stainless steel reservoirs of various volumes which feed into a manifold with an in-line step-down pressure regulator which controls the pressure of propylene being fed into the reactor. The pressure inside the manifold is monitored by a pressure gauge

---

[64] The response of the pentad distribution to using 2D-propene might prove instructive.

[65] Hu, Y.; Krejchi, M. T.; Shah, C. D.; Myers, C. L.; Waymouth, R. M. *Macromolecules* **1998**, *31*, 6908−6916.

[66] Hu, Y.; Carlson, E. D.; Fuller, G. G.; Waymouth, R. M. *Macromolecules* **1999**, *32*, 3334−3340.

[67] Carlson, E. D.; Fuller, G. G.; Waymouth, R. M. *Macromolecules* **1999**, *32*, 8100−8106.

[68] Carlson, E. D.; Fuller, G. G.; Waymouth, R. M. *Macromolecules* **1999**, *32*, 8094−8099.

connected to a computer. Gas reservoirs were calibrated using helium and a reservoir of known volume. The reservoir pressure was logged during a solubility or polymerization experiment using the Strawberry Tree Data Acquisition Program. Data were evaluated using Kaleidagraph.

Measurement of Propylene Solubilities. A 100 mL toluene solution was charged into a 300 mL stainless steel reactor, the headspace above the solution was flushed with dry Ar and left under 1 atm of Ar, and the stirred solution was brought to the desired temperature using a heater and/or cooling loop. Then, (1) the regulator on the kinetics apparatus was set to the desired pressure (typically starting at 10 psig) and the stirrer was turned off, (2) the headspace of the reactor was pressurized, which caused a decrease in the pressure in the reservoir, and (3) after waiting 1 min for the pressure to stabilize, the stirrer was started and propylene consumption by the solution was monitored by watching the pressure drop in the reservoir. Once propylene consumption had ceased, the stirrer was stopped and the regulator set to a higher pressure (typically a 10 psig step (0.68 atm)). Then steps 2 and 3 were repeated.

The amount of propylene dissolved in the solution was calculated from the pressure of the reservoir when the stirrer was started and the pressure of the reservoir when gas was no longer being consumed. The number of moles was calculated using the van der Waals equation[69] (eq 7),

$$(P + a(n/V)^2)((V - nb)) = nRT \qquad (7)$$

where $a = 123.1373$ L^2 psi/(mol K); $b = 0.0827$ L/mol; $R = 1.206\,282$ L psi/(mol K).[70] The number of moles in solution at any given pressure is the sum of the number of moles absorbed by the solution in each 10 psig pressure step (the total number of moles in solution at 30 psig is equal to (number of moles absorbed on going from 0 to 10 psig) + (number of moles absorbed on going from 10 to 20 psig) + (number of moles absorbed on going from 20 to 30 psig). The volume of the solution at any given pressure is then calculated using the measurements described below. The solubility of propylene is plotted versus the partial pressure of propylene inside the reactor, subtracting the partial pressure of Ar (1 atm) and the toluene vapor pressure[71] from the total pressure.

Measurement of Solvent Volume. A 50 mL portion of toluene was placed in a glass Fisher-Porter bottle equipped with a large magnetic stir bar and placed in a water bath at the desired temperature. The headspace above the solution was flushed using dry Ar and left under 1 atm of Ar. The regulator on the kinetics apparatus was set to the desired pressure (typically starting at 10 psig) and the bottle pressurized with stirring. The pressure in the reservoir was monitored until propylene consumption ceased. The volume of the solvent was then recorded. The regulator was then increased by 10 psig and the propylene consumption monitored again. A plot of solvent volume versus propylene pressure (taking into account the 1 atm of Ar initially inside the Fisher-Porter bottle) yielded a curve which was fitted using Kaleidagraph and used to determine volume at any pressure.

Calculation of k_La. The mass-transfer coefficient was determined by logging the pressure in the propylene reservoir every 10−30 s after the stirrer had been turned on; the stirrer speed was 1460 rpm. The mass-transfer coefficients were calculated according to eq 1,

$$\frac{P_2 - P_0}{P_1 - P_0} \ln \frac{P_1 - P_2}{P_t - P_2} = k_L a t \qquad (1)$$

where P_1 = initial pressure in the reservoir, P_2 = final pressure in the reservoir, P_0 = presaturation pressure, and P_t = pressure in the reservoir at time t. The presaturation pressure P_0 was taken to be the pressure in the reactor before the regulator pressure was increased and the headspace of the reactor was pressurized (i.e., when calculating the k_La on going from 60 to 70 psig, P_0 = 60 psig). The mass-transfer coefficient, k_La, is determined from the slope of the line obtained by plotting the left-hand side of the equation versus t for data points collected in the first 5−10 min of propylene uptake.

Error Analysis. Errors for propylene solubility were calculated by determining the linear fit to the solubilities measured for each different solubility run (five for toluene at 20 °C). Those equations were then used to solve for the solubility at propylene partial pressures of 0.68−5.58 atm. The standard deviations of those solubilities are the errors reported.

A second method for estimating the error is propagation of uncertainties. In the calculation of the number of moles dissolved, the uncertainties in pressure P of ±1 psig, reservoir volume V of ±0.005 L, and temperature T of ±1 K were used. The uncertainty in the number of moles could then be calculated as

$$\frac{\partial n}{|n|} = \left[\left(\frac{\partial P}{P}\right)^2 + \left(\frac{\partial T}{T}\right)^2 + \left(\frac{\partial V}{V}\right)^2\right]^{1/2} \qquad (8)$$

For P = 70 psig, T = 295 K, V = 0.450 L, and n = 0.088 mol, $\delta n = \pm 0.002$ mol. The error in the toluene volume is ±0.005 L. Therefore, the error in the solubility (as calculated by n/V_{tol}) is 0.05 M at 5 M. This is in reasonable agreement with the value estimated from the first method.

The uncertainty in the rate of polymerization from propagation of error is also ±0.002 mol from the calculation above. However, the mass balance between the amount of monomer consumed and the amount of polymer isolated is in general greater than this (±0.01 mol), and that is the error that is considered in polymerizations.

General Procedure for Propylene Polymerizations. Prior to the beginning of the polymerizations each day, the drybox was purged with nitrogen for 5 min; [O_2] ≈ 0−2 ppm. A 300 mL stainless steel reactor bottom and stirrer were baked in a 110 °C glassware oven, and the assembled reactor was then pumped down to <60 mTorr on a vacuum line and refilled with dry N_2. The reactor was then purged with propylene. The metallocene and MAO were weighed using a Mettler Toledo AB204 balance. Metallocene solutions were measured using a 1000 μL Pipetman.

MAO was dissolved in 18 mL of toluene and stirred for 60−75 min. This solution was added to 80 mL of toluene in a 150 mL stainless steel injection tube and placed into the reactor under propylene pressure at the pressure of the polymerization to be performed. The MAO/toluene solution was equilibrated at the polymerization pressure for 60−75 min with stirring at maximum speed (1460 rpm). Propylene uptake was monitored using the reservoir on the kinetics apparatus. When propylene uptake was complete, the reactor stirrer was turned off and the hose from the kinetics apparatus was detached and used as described below.

Catalyst solutions were prepared and used for a set of four polymerizations. Between polymerizations, the solutions were kept in the drybox freezer to prevent decomposition. Approximately 15 min prior to loading of the metallocene solution into the injection tube, the solutions were stirred and warmed to the box temperature. An aliquot of the solution was placed in an 8 mL stainless steel injection tube, and toluene was added to this to make the total volume of the solution equal to 2 mL. This 2 mL solution was saturated with propylene at the polymerization pressure by connecting the tube to the propylene source and shaking vigorously until propylene uptake from the reservoir ceased.

To inject the metallocene, all three reservoirs (see Figure 12) were filled to maximum propylene pressure and then isolated from the propylene source. The stirrer of the reactor was turned off, and the data log was started. The reactor headspace was vented down to 0.34 atm (5−6 psig) less than the polymerization pressure, and the catalyst injection tube (at the polymerization pressure from the reservoirs) was connected to the reactor liquid injection port. The stirrer was then started and maintained at 1460 rpm. During the first minute of polymerization, the catalyst injection tube was removed from the reactor. After 1 min the 2 L reservoir and either the 300 mL or 1 L reservoir were closed off such that only one reservoir was providing propylene to the polymerization. The pressure inside this reservoir was recorded every

---

[69] The pressure of propylene in the reservoirs was close to the vapor pressure of liquid propylene. At such high pressures, the van der Waals equation is the more appropriate equation of state to use in the calculation of the number of moles rather than the ideal gas law. The solubilities calculated using the van der Waals equation were also more consistent with the values reported in ref 45.

[70] *CRC Handbook of Chemistry and Physics*, 63rd ed.; Weast, R. C., Ed.; CRC Press Inc: Boca Raton, FL, 1983; Vol. 63.

[71] Munday, E. B.; Mullins, J. C.; Edie, D. D. *J. Chem. Eng. Data* **1980**, *25*, 191−194.

30 s for the duration of the polymerization. The metallocene concentration was adjusted such that the maximum rate of polymerization was approximately an order of magnitude less than the diffusion rates measured for 100 mL of toluene (initial volume) at 20 °C with no polymer in the solvent. In addition, the amount of polymer isolated was compared to the amount of propylene consumed, and agreement in these values was taken as another indication that the rate of polymerization was less than the measured rate of diffusion (vide supra).[72] The amount of polymer isolated was within 200 mg or 15% of the amount of monomer consumed in all cases.

The polymerization was quenched using 10 mL of methanol delivered under Ar pressure. The reactor was vented down to atmospheric pressure, and the resulting toluene/methanol solution was added to 500 mL of acidic methanol to precipitate the polymer. After the resulting solution was stirred overnight, the polymer was recovered via filtration and dried in a 40 °C vacuum oven for several hours.

Polymer Characterization. ^{13}C NMR spectra of the polymers synthesized were collected using a 75 MHz Varian Inova spectrometer. Samples were prepared using $C_2H_2Cl_4/C_2D_2Cl_4$, and data were collected at 100 °C.

Polymer MWs were measured using a Waters 150-C ALC/GPC at 139 °C equipped with two Polymer Laboratories PLgel 10 μM mixed B-(AM) columns. Sample solutions of 0.067% (wt/vol) are typically prepared by weighing 20 mg of sample and 12−15 mg of Santanox R antioxidant (Monsanto) into a 36 mL screw cap vial. To each vial is added 30 mL of 1,2,4 trichlorobenzene (TCB) (*caution: TCB is toxic*), and a blanket of argon is applied. The vials are sealed with Teflon-lined steel caps and tumbled at 10 rpm for at least 4 h in a forced draft oven set at 145 °C. The sample solutions are then filtered through a 0.5 μm Teflon membrane maintained at 150 ± 10 °C and poured into 4 mL vials, positioned in a heated sand bath, before being returned to the oven and the sample carriage that will be placed into the Waters 150C injector compartment for autosampling. A 300 μL injection volume is used. The TCB mobile phase is not stabilized. A broad MW standard calibration based on a well-characterized commercial grade PP is used. The established cumulative weight percent distribution for the calibration standard was fitted with average elution times for a series of standards associated with a GPC run. The resulting elution time vs log MW distribution equates the current calibration standard data to the established standard values. It is then fitted with a fifth-order polynomial that describes the calibration curve (cc). A low-MW material, *n*-tetracontane, is measured to establish a point at the PP equivalent MW of 851, and both ends of the cc are fixed by linear extrapolation for consistency. Statistical data for the PP calibration standard follow. They represent the average of more than 800 measurements each. $M_n = 95\,700 \pm 2480$, $M_w = 537\,000 \pm 4910$, $M_z = 1\,605\,000 \pm 32\,100$, $M_{z+1} = 3\,114\,000 \pm 129\,000$, and $M_w/M_n = 5.61 \pm 0.14$.

DSC measurements were obtained using the Perkin-Elmer DSC 7 instrument. Samples of polymer (7−9 mg) were annealed at 180 °C for 10 min, cooled to 25 °C at 10 °C/min, and then aged at room temperature for 5 weeks; the rate of heating was 20 °C/min.

Acknowledgment. We acknowledge BPAmoco and the NSF (Grant CHE-9615699) for financial support. S.L. is the recipient of the Veatch Memorial Fellowship for which she is grateful. C.D.T. thanks the NIH for National Research Service Award No. 5,F32GM17850-02. We thank Dr. Paul Tindall of Experimental Equipment Design for the design of the kinetics apparatus, him and Dr. Eric Carlson for helpful discussion, and BPAmoco for high-temperature GPC measurements.

Supporting Information Available: Tables of diffusion rates of propylene into toluene and the increase in volume of the toluene solution with propylene uptake (PDF). This material is available free of charge via the Internet at http://pubs.acs.org.

JA002003H

---

(72) The polymerization conditions used started with a toluene solution saturated at the propylene pressure for the polymerization. A rate of polymerization faster than the rate of diffusion would result in some amount of propylene taken out of solution, which was not replaced by gaseous monomer diffusing into solution. The result would be a greater amount of polymer isolated than monomer consumed.